[Frontiers In Bioscience, Scholar, 11, 1-8, Jan 1, 2019]

Nigral injection of 6-hydroxydopamine induces changes in spatial arrangement of striatal neuron and glial cells

Vahid Ebrahimi[1], Abbas Aliaghaei[1], Abbas Piryaei[1,2], Hossein Haghir[3,4,5], Mohammad-Amin Abdollahifar[1*], Yousef Sadeghi[1*]

[1]Department of Biology and Anatomical Sciences, School of Medicine, Shahid Beheshti University of Medical Sciences, Tehran, Iran, [2]Department of Tissue Engineering and Applied Cell Sciences, School of Advanced Technologies in Medicine, Shahid Beheshti University of Medical Sciences, Tehran, Iran, [3]Department of Anatomy, Faculty of Medicine, Mashhad University of Medical Sciences, Mashhad, Iran, [4]Medical Genetic Research Center (MGRC), Mashhad University of Medical Sciences, Mashhad, Iran, [5]Institute of Neuroscience and Medicine (INM-1), Research Center Julich, Julich, Germany

TABLE OF CONTENTS

1. ABSTRACT

In Parkinson's disease, nigral dopamine neurons are lost and the structure of the striatum is progressively degraded. These events lead to a substantial neuronal loss in the striatum, changing spatial pattern of the neurons and glial cells, and associated cellular connections. Therefore, the aim of this study was to develop a new insight into whether the Parkinson's disease causes a change in the spatial arrangement of the neurons and glial cells in the striatum. Nigral injection of 6-hydroxydopamine led to a significant reduction in the total number of the neurons, an increase in the number of striatal glial cells, and disruption in the spatial arrangement of glial and neuronal cells in the Parkinson's disease-induced group, compared to the control group. The data support the idea that in Parkinson's disease, the function of the

striatum is disturbed by both the loss of neurons and an increase in the number of glial cells, culminating in the disordered spatial distribution of these cells.

2. INTRODUCTION

Parkinson's disease (PD) is known as a common neurological syndrome. This condition affects the life of many patients around the world and eventually can lead to a variety of motor coordination impairments and disabilities (1). The manifestation of disease depends on different causes, but what it is certain is that gradual degradation of dopamine (DA) producing neurons in the midbrain is responsible for incidence of symptoms (2). Indeed, massive neuronal death in both substantia nigra (SN) and the striatum, as the main target tissue of the DA cells, is one of the most significant factors involved in the pathogenesis of disease (3). Complicated structural, histological, and molecular alterations in SN and striatum, deterioration of nigrostriatal pathway and the decline of the neurotransmitter in the striatum occur, following the destruction of the DA cells (4, 5).

Nowadays, many researchers in the field of medicine and neurological disorders are still looking for effective cures for patients with PD (6). Therefore, understanding the initial processes in the progression of disease in the central nervous system can help, in taking the confident treatment approaches for improving neural function.

Many interactions between neuron and glial cells are regulated by signaling pathway. However, attention has recently shifted to identifying the spatial arrangement of cells, because this information will be useful in clarifying, the mechanisms of cell to cell interactions. Impairment of these properties dictates many of the neurological conditions (7).

Stereological techniques can provide further valuable information about the structural changes and spatial arrangement in normal and pathologic conditions, such as neurodegenerative disorders. Our goal is to better understand the effects of 6-hydroxydopamin (6-OHDA) on histological structure. Accordingly, in this study stereological methods were used to address the following questions: What changes occur in the spatial arrangement of striatal neurons and glial cells, after injection of 6-OHDA? In addition, will the number of the neurons and glial cells change, after injection of 6-OHDA in rats?

3. MATERIALS AND METHODS

3.1. Animals

In this study, eighteen adult male Sprague–Dawley rats (250±20g) were obtained from the laboratory animal center of Shahid Beheshti University of Medical Sciences, Tehran, Iran. The animal experiments were approved by the Ethics Committee of the University (IR.SBMU. MSP. REC.1395.3.20). Rats were considered randomly into two main experimental groups; the first one, control group (with no surgical or injection procedure, n=9) and the second one, 6-OHDA group (rats under injection of neurotoxin, n=9). Animals were housed under standard conditions, room temperature (22–24°C), 12:12 h light-dark schedule and free access to water and food.

3.2. Simulation of experimental model of PD

The animals were anesthetized intraperitoneally with a mixture (1 ml/kg), containing 9 mg/kg xylazine and 90 mg/kg ketamine. Then, induction of the PD model in animals was performed by a single dose injection of 4µg of 6-OHDA (Sigma, USA), in 2µl of physiological saline, containing 0.02% ascorbic acid into the right SN, using a unilateral stereotaxic injection with a Hamilton microsyringe (8). Coordinates were set according to the atlas of Paxinos and Watson (9), using the following coordinates: anteroposterior (AP): 4.3. mm, lateral (L): 1.6. mm, and Dorsoventral (DV): 8.2. mm.

3.3. Apomorphine turning behavior

In order to ensure the proper induction of PD, apomorphine-induced turning behavior is performed for all animals. Accordingly, the animals received a subcutaneous injection (0.05 mg/kg of apomorphine hydrochloride (Sigma, USA) dissolved in 1% ascorbic acid and 0.9% NaCl) in the neck, and placed on metal testing bowls for 30 minutes. Then, the number of contralateral rotations was digitally recorded and analyzed.

3.4. Tissue preparation

Rats were deeply anesthetized and sacrificed with sodium pentobarbital intraperitoneally (Eutasil, 60 mg/kg). After that, trascardial perfusion was performed using chilled normal saline and fresh fixative solution, containing 4% paraformaldehyde (PFA) in 0.1M Phosphate buffered saline (PBS). All animal brains were exposed by a midline incision along the skull, then the brains were dissected, and immediately immersed in a 10% fresh formalin solution for one week. Subsequently, the samples were embedded in paraffin blocks. Eventually, the complete serial sections (5-10 µm), using a microtome were prepared for stereological study. Every 10 sections were sampled, starting with a random number between 1 and 10. Then, approximately 8–10 tissue sections of each animal were selected in a systematic random manner. The selected sections were stained with Haematoxylin and Eosin (H&E) and analyzed.

3.5. Estimation of the number of the neurons and glial cells

The total number of the neurons and glial cells in the striatum was determined using the optical disector method. The positions of the microscopic fields were selected by an equal interval of moving the stage and systematic uniform random sampling (SURS). Microcator was used for measurement of Z-axis movement of the microscope stage. An unbiased counting frame with inclusion and exclusion borders was superimposed on the images of the sections, viewed on the monitor. A nucleus was counted, if it was placed completely or partially within the counting frame and did not reach the exclusion line. Numerical density (N_v) was calculated with the following formula:

$$N_v = \frac{\sum Q}{\sum P \times h \times \frac{a}{f}} \times \frac{t}{BA}$$

Where *"ΣQ"* is the number of the nuclei, *"ΣP"* is the total number of the unbiased counting frame in all fields, *"h"* is the height of the dissector, *"$\frac{a}{f}$"* is the frame area, *"t"* is the real section thickness measured in every field using the microcator, and *"BA"* is the block advance of the microtome which was set at 10µm. The total number of the neuron and glial cells was estimated by multiplying the numerical density (N_v) by the total V (10).

$$N_{total} = N_v \times V$$

3.6. Estimation of the coefficient of error (CE)

The CE for the estimate of the volume; i.e., CE (V), was calculated by the following formula:

$$\frac{1}{240\left(3\sum P_i^2 + \sum P_i P_{i+2} - 4\sum P_i P_{i+1} + 0.0724 + \frac{B}{\sqrt{A}} \times \sqrt{n\sum P_i}\right)_{1/2}}$$

Where "B" and "A" represented the mean section boundary length and mean sectional area, respectively. The CE for the estimate of the total neuron and glial cell number, CE (N), was derived from CE (V) and CE (N_v) using the following formula (11):

$$CE(N) = \left[CE^2(N_v) + CE^2(V)\right]_{1/2}$$

$$CE(N_v) = \left[\left(\frac{n}{n-1}\right) \times \left[\left(\frac{\sum(Q)^2}{(\sum Q)^2}\right) + \left(\frac{\sum(P)^2}{(\sum P)^2}\right) - \left(\frac{2\sum(QP)}{(\sum Q \sum P)}\right)\right]\right]_{1/2}$$

The CE have been shown in Table 1.

3.7. Estimation of the covariance function

A transparent lattice bearing one row of points was designed to serve as a set of linear dipole probes (12). Each row composed of 50 points and 49 equidistant intervals. The point interval corresponded to a distance of 2.6. µm on the scale of the specimen. Consequently, both end points of dipoles (DP) of class size r = 1 (equivalent to 2.6. µm) had the chance of being included within the same profile of the glial cells. The lattice was superimposed on the live Figure (4 D) on a monitor connected to a microscope. For each striatum, 11 trials (a total of p = 550 test points) were conducted. For every trial, the nature of the tissue component underlying each test point was noted and all the information was recorded on a 50 × 11 matrix. Within the cells of this matrix, each test point was coded as 1 (neuron), 2 (glia), and 3 (neuropil). To estimate "C (r)", and "g (r)", the distance between the points (DP) ranged from r = 0 (equivalent to 0 µm) to r = 49; so, the total distance was 127.4. µm (49 × 2.6. = 127.4. µm) (13-17). The covariance of a component (X) was estimated using the following equation:

$$\mathrm{C\ (r)X} = \frac{\sum DP(X,r)}{\sum DP(ref,r)}$$

3.8. Estimation of the pair correlation function

Pair correlation function is the normalized covariance function obtained by dividing the covariance by the reference value (12):

$$\mathrm{g\ (r)} = \frac{C(r)}{Vv2}$$

3.9. Estimation of the cross-covariance function

All the above descriptions refer to the covariance for a single component with its counterpart. In a multi-component tissue, dipoles often hit two different phases simultaneously (12). The function used to quantify spatial arrangement is cross-covariance (C (r)X,Y) and can be estimated using the equation:

Table 1. Coefficients of error (CE) for total volume, neuronal and glial numbers as well as neuronal and glial densities in the striatum

Groups	Striatum Volume	Neuron Density	Neuron Number	Glia Density	Glia Number
Control	0.05	0.04	0.05	0.05	0.04
6-OHDA	0.03	0.04	0.03	0.05	0.03
6-OHDA+Cell	0.04	0.03	0.05	0.03	0.03

$$C\ (r)X,Y = \frac{\sum DP(XY,r)}{\sum DP(ref,r)}$$

3.10. Estimation of the cross-correlation function

The cross-covariance between the two different components of X and Y is defined as the probability that an isotropic dipole of length "r" units hits components X and Y simultaneously divided by the number of dipoles hitting the reference volume. Similarly, the cross-covariance can be normalized to take out volume fraction differences using the estimation of cross-correlation functions and the following equation:

$$g\ (r)X,Y = \frac{C(r)XY}{Vv(X,ref)\times Vv(Y,ref)}$$

3.11. Statistical analysis

The analysis was carried out 'pointwise' methods for comparing complete co-variograms. Comparisons of g (r) of motor neuron and glial cells and cross-correlation between the groups were undertaken using Mann–Whitney U-tests. Besides, p ≤ 0.0.5 was considered as statistically significant.

4. RESULTS

4.1. Injection of 6-OHDA into the SN induced Apomorphine-dependent rotations

The results obtained from apomorphine-induced rotation test showed 6-OHDA-lesioned animals, presenting more than 100 rotations in 30 minutes, were considered to have a nearly complete lesion whereas, the control animals showed less than 10 rotations. Statistical analysis revealed differences in apomorphine-induced turning behavior, demonstrating a significant higher number of rotations in the 6-OHDA group, compared to the control group rats (p<0.0.5) (Figure 1).

4.2. 6-OHDA administration caused a significant decrease in the number of the neurons, whereas it increased the number of glial cells

Our results showed a significant reduction in the total number of the neurons in the 6-OHDA group, compared to the control group (P<0.0.5) (Figure 2, A and C). In addition, we observed an increase in the number of striatal glial cells in the 6-OHDA group, in comparison with the control group (P<0.0.5) (Figure 2, B and C).

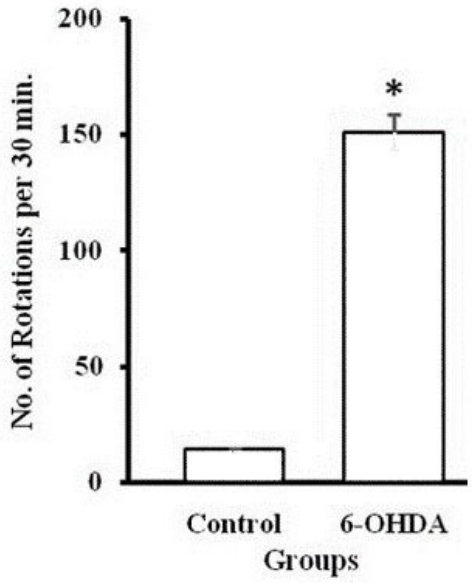

Figure 1. Apomorphine-induced turning behavior revealed intense contralateral rotations in 6-OHDA lesioned animals compared to the control animals, with a few normal turning behaviors (* represents p<0.05).

4.3. Spatial arrangement of the neurons and glial cells was changed following injection of 6-OHDA (Convert a data matrix to image type using MAT-LAB software)

The spatial arrangement of the neurons and glial cells was changed by injection of 6-OHDA, and dissociation of the neurons and glial cells could be seen in some places. This indicates that the neurons and glial cells are not normally arranged after injection of 6-OHDA. For better understanding of the images, cell arrangements were presented in the figures 3 A and B, show the arrangement of the neurons and glial cells in the control (A) and 6-OHDA (B) groups.

4.4 Spatial arrangement of the neurons

Estimation of g (r) for the neurons are plotted against the dipole distances, r, in figure 4A. The values at the beginning of the curve (from r=0 to 10.4. µm), (from r=15.6. to 62.4. µm), (from (from r=109.2. to 114.4. µm), (from r=119.6. to 124.8. µm) showed a difference between the control (A) and6- OHDA groups. After the gap, the data points in both groups showed a random arrangement at larger distances (p<0.0.5).

4.5. Spatial arrangement of the glial cells

Estimattion of g (r) for the glial cells are plotted against the dipole distances, r, in figure 4B. The values at the beginning of the curve (from r=0 to 7.8. µm), (from r=13 to 28.6. µm), (from r=31.2. to 39 µm)

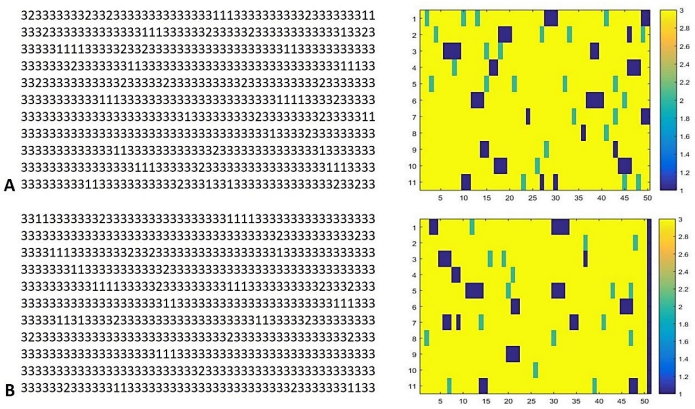

Figure 2. The total number of the neurons (A) and glial cells (B) in the 6-OHDA and control rats were compared. (C) The light photomicrograph of striatum (H&E staining); N: Neuron, G: Glial cell. Each test point was coded as 1, 2, and 3, if the point was laid on the neurons (1), glial (2), and neuropil (3), respectively.

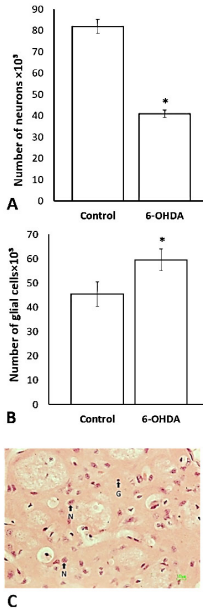

Figure 3. A data matrix conversion to image type. The neurons (1) are shown in dark blue, glial cells (2) are shown in light blue, and neuropil (3) is shown in yellow. (A): control group and (B): 6-OHDA group.

and (from r=46.8. to 65 µm), (from r=72.8. to 122.2. µm) showed a difference between the control (A) and6- OHDA groups. After the gap, the data points in both groups showed a random arrangement at larger distances (p<0.0.5).

4.6. Cross-correlation of the neurons and glial cells

In the figure 4C, some differences in the spatial arrangement of the neurons and glial cells were showed by plotting the cross-correlation function versus distance. The results indicated a negative correlation between the neurons and glial cells at 0-127.4. µm also, a negative correlation was observed at 106.6.-127.4. µm in the control group, in comparison with the 6-OHDA group (p<0.0.5).

5. DISCUSSION

The spatial arrangement of the cells is highly associated with correlation and interactions between the cells. There is a hypothesis that spatial cell organization related to induce signaling and coordinates cellular behavior. Cell-cell interactions drive numerous physiological processes, and help coordinate functioning, in multicellular organisms. We propose a new view of the cellular spatial arrangement. This different view describes cell to cell interactions related to the normal function and pathological conditions of the organ. However, Alterations in these cell-cell interactions, may cause abnormal tissue physiology associated with disease states (18, 19).

Initially, behavioral test and furthermore histological results indicated that injection of the 6-OHDA to the SN could induce Parkinson's model in rats. In this study, we obtained an accurate evaluation and a unique quantitative analysis of the cellular spatial design, in the striatum of a rat model of PD. The present study showed the quantitative alterations in spatial distributions of the neurons and glial cells within the striatum, using second-order stereology method. Our current research also investigated the changes in the total number of the neurons and glial cells in the striatum, following injection of 6-OHDA, using a new approach based on stereological methods.

According to the acquired results, the plots of pair-correlation function of neurons and glial cells, indicated variation in the arrangement of neurons and glial cells, and wider gaps in neuron and glial cells in the 6-OHDA-lesioned rats. Moreover, the cross-correlation function showed a negative correlation between the neurons and glial cells in 6-OHDA rats.

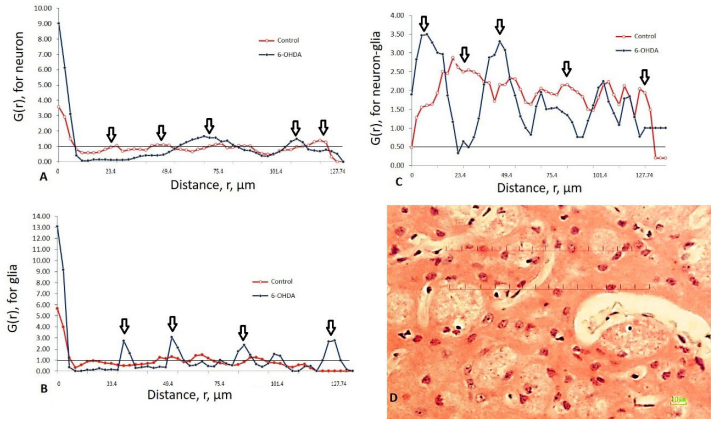

Figure 4. (A): Relationship between pair correlation function and dipole distance for neurons in the control and 6-OHDA groups. (B): Relationship between pair correlation function and dipole distance for glial cells in control and 6-OHDA groups. (C): The cross-correlation function, g (r), between the neurons and glial cells plotted versus distance, r, in micrometers. The dots are the mean g (r) across the five animals in the control and 6-OHDA groups. The horizontal reference line corresponds to values expected for a random spatial arrangement (g (r)=1). Arrows indicate significant differences. The arrow (↓) indicates the value of the distance for which there was a significant difference of cross-correlation function. (D): A photomicrograph stained with H&E, illustrates a transparent lattice of points was constructed to serve as a set of dipole probes. The point interval (r) corresponds to a distance of 2.6 µm.

However, these gaps can be filled with neuropil. It can be a reason for altered spatial distributions of the cells in the current study. These data were in conformity with our previous study, indicating alterations in the neurons, glial cells, and Purkinje cells arrangement (20, 21).

The glial cell activation is a prominent neuropathological feature of various neurological diseases, specifically PD. This alteration in the number of the neurons and glial cells was accompanied by changes in spatial distributions of cells in the striatum and it was in accordance with other works, explaining the structural changes in the striatum, followed by injection of 6-OHDA (22, 23).

Several mechanisms might be responsible for the disturbance in the spatial arrangement of neurons and glial cells in the striatum of Parkinsonian rat. In previous investigations, it was revealed that in the final stages of PD, accumulation of abnormal metabolites can be found even in the residual neurons, due to the death of impaired neurons and also the increase in glial cells number. Administration of 6-OHDA into the SN, also provokes degeneration of neurons possibly due to the generation of reactive oxygen species (ROS) and as a result, cytotoxicity related to oxidative stress is increased in the damaged brain. Moreover, decreasing in the number of neurons could be elicited by apoptosis and necrosis in the striatum, after injection of 6-OHDA (22, 23).

There are several reports of morphometry techniques to detect the volume decrease in brain striatum, brain stem, limbic structures, and brain cortex in PD patients. Hikishima et al. indicated volume decreases in the SN of the MPTP-induced marmoset model of PD, using MRI histology methods (24). Burton et al. showed that the volume of grey matter in PD patients has significant reductions in the temporal and frontal lobes, compared with the healthy persons (25). Camicioli et al. presented that progression of motor signs and movement impairments in PD were associated with morphological atrophy in the brain striatum and cortex (26).

Thus, the data provide important additional information about the distribution of neurons and glial cells in the neurodegenerative disorders particularly, PD.

6. CONCLUSION

In general, to the best of our knowledge, this is the first report to use the stereological assessments, regarding major alterations in the spatial arrangement of neuron and glial cell in PD. The outcomes of this study suggest destructive impacts of PD, on the spatial design and the connections of neurons. Our data suggest that impaired striatal cell-cell interaction may contribute to one of the pathogenesis of Parkinson's disease because the normal communication between striatal cells to be essential for normal function of neurons in striatum. Further examination of the cellular and molecular biology of abnormal tissue is speculated to reveal that many complications may be associated with cell-cell interactions. The results of this study pave the way for a greater clinical perspective for identification of the effects of PD on the nervous system.

7. ACKNOWLEDGMENTS

This research was supported financially by the Vice chancellor for Research of Shahid Beheshti University of Medical Sciences, Tehran, Iran (Grant

No. 94-366). This study also is a part of the thesis written by Vahid Ebrahimi, Ph.D student of Anatomical Sciences. The authors declare that they have no conflict of interest.

8. REFERENCES

1. DB Miller, JP O'Callaghan: Biomarkers of Parkinson's disease: present and future. *Metab Clin Exp* 64, 40-46 (2015). https://doi.org/10.1016/j.metabol.2014.10.030

2. F Han, D Baremberg, J Gao: Development of stem cell-based therapy for Parkinson's disease. *Transl Neurodegener* 4, 16-28 (2015). https://doi.org/10.1186/s40035-015-0039-8

3. PP Michel, EC Hirsch, S Hunot: Understanding dopaminergic cell death pathways in Parkinson disease. *Neuron* 90, 675-691 (2016). https://doi.org/10.1016/j.neuron.2016.03.038

4. I García-García, Y Zeighami, A Dagher: Reward prediction errors in drug addiction and Parkinson's disease: from Neurophysiology to Neuroimaging. *Curr Neurol Neurosci Rep* 17, 46-55 (2017). https://doi.org/10.1007/s11910-017-0755-9

5. AA Kehagia, RA Barker, TW Robbins: Neuropsychological and clinical heterogeneity of cognitive impairment and dementia in patients with Parkinson's disease. *Lancet Neurol* 9, 1200-1213 (2010). https://doi.org/10.1016/S1474-4422(10)70212-X

6. CW Olanow, MB Stern, K. Sethi: The scientific and clinical basis for the treatment of Parkinson disease.*Neurology* 72, 1-136 (2009). https://doi.org/10.1212/WNL.0b013e3181a1d44c

7. H Lian, H Zheng: Signaling pathways regulating neuron-glia interaction and their implications in Alzheimer's disease. J Neurochem 136, 475-491 (2016). https://doi.org/10.1111/jnc.13424

8. BS Jeon, V Jackson-Lewis, RE Burke: 6-hydroxydopamine lesion of the rat substantia nigra: Time course and morphology of cell death. *Neurodegeneration* 4, 131–137 (1995). https://doi.org/10.1006/neur.1995.0016

9. G Paxinos, C Watson. The Rat Brain in Stereotaxic Coordinates, Press Inc, New York, (1986)

10. A Noorafshan, MA Abdollahifar, R Asadi-Golshan: Curcumin and sertraline prevent the reduction of the number of neurons and glial cells and the volume of rats' medial prefrontal cortex induced by stress. *Acta Neurobiol Exp* 74, 44-53 (2014). http://www.ane.pl/home.php. 1689-0035

11. HJ Gundersen, EB Jensen: The efficiency of systematic sampling in stereology and its prediction. *J Microsc* 147, 229–263 (1987). https://doi.org/10.1111/j.1365-2818.1987.tb02837.x

12. TM Mayhew: Quantitative description of the spatial arrangement of organelles in a polarised secretory epithelial cell: the salivary gland acinar cell. *J Anat* 194, 279-285 (1999). http://www.ncbi.nlm.nih.gov/pmc/journals/265/

13. RA Krasnoperov. D Stoyan: Second-order stereology of spatial fibre systems. *J Microsc* 216, 156-164 (2004). https://doi.org/10.1111/j.0022-2720.2004.01407.x

14. MG Reed, CV Howard, GS Yanés: One-stop stereology: the estimation of 3D parameters using isotropic rulers. *J Microsc* 239, 54-65 (2010). https://doi.org/10.1111/j.1365-2818.2009.03356.x

15. TM Mayhew: Second-order stereology and ultrastructural examination of the spatial arrangements of tissue compartments within glomeruli of normal and diabetic kidneys. *J Microsc* 195, 87-95 (1999). https://doi.org/10.1046/j.1365-2818.1999.00593.x

16. T Mattfeldt T, S Eckel, F Fleischer: Statistical analysis of reduced pair correlation functions of capillaries in the prostate gland. *J Microsc* 223, 107-119 (2006). https://doi.org/10.1111/j.1365-2818.2006.01604.x

17. T Mattfeldt, H Frey, C Rose: Second-order stereology of benign and malignant alterations of the human mammary gland. *J Microsc* 171, 143-151 (1993). https://doi.org/10.1111/j.1365-2818.1993.tb03368.x

18. B L.Ekerdt, R A.Segalman, D V.Schaffer: Spatial organization of cell-adhesive ligands for advanced cell culture. Biotechnol J 8, 1411-1423 (2013). https://doi.org/10.1002/biot.201300302

19. L Altomare, S Farè: Cells response to topographic and chemical micropatterns. J Appl Biomater Funct Mater 6, 132–143 (2008). https://doi.org/10.1177/228080000800600302

20. A Noorafshan, MA Abdollahifar, S Karbalay-Doust: Stress changes the spatial arrangement of neurons and glial cells of medial prefrontal cortex

and sertraline and curcumin prevent it. *Psychiatry Investig* 12, 73-80 (2015)

21. R Mohammadi, MH Heidari, Y Sadeghi, MA Abdollahifar, A Aghaei: Evaluation of the spatial arrangement of Purkinje cells in ataxic rat's cerebellum after Sertoli cells transplantation. *Folia Morphol* 77,194-200 (2018). https://doi.org/10.5603/FM.a2017.0091

22. P Damier, EC Hirsch, P Zhang, Y Agid, F Javoy-Agid: Glutathione peroxidase, glial cells and Parkinson's disease. *Neuroscience* 52, 1-6 (1993). https://doi.org/10.1016/0306-4522(93)90175-F

23. A Benazzouz, B Piallat, ZG Ni, A Koudsie, P Pollak, AL Benabid: Implication of the subthalamic nucleus in the pathophysiology and pathogenesis of Parkinson's disease. *Cell Transplant* 9, 215-221 (2000). http://journals.sagepub.com/home/cll https://www.ncbi.nlm.nih.gov/pmc/journals/3327/

24. K Hikishima, K Ando, Y Komaki, K Kawai, R Yano, T Inoue, T Itoh, M Yamada, S Momoshima, HJ Okano: H Okano: Voxel-based morphometry of the marmoset brain: In vivo detection of volume loss in the substantia nigra of the MPTP-treated Parkinson's disease model. *Neuroscience* 300, 585-592 (2015). https://doi.org/10.1016/j.neuroscience.2015.05.041

25. EJ Burton, IG McKeith, DJ Burn, ED Williams, JT O'Brien: Cerebral atrophy in Parkinson's disease with and without dementia: a comparison with Alzheimer's disease, dementia with Lewy bodies and controls. *Brain* 127, 791-800 (2004). https://doi.org/10.1093/brain/awh088

26. R Camicioli, M Gee, TP Bouchard, NJ Fisher, C CHanstock, DJ Emery: Voxel-based morphometry reveals extra-nigral atrophy patterns associated with dopamine refractory cognitive and motor impairment in parkinsonism. *Parkinsonism Relat Disord* 15, 187–195 (2009). https://doi.org/10.1016/j.parkreldis.2008.05.002

Abbreviations: SN: substantia nigra, PD: Para kinson's disease,6-OHDA: 6-hydroxydopamin, ROS: reactive oxygen species DA: dopamine, Nv: Numerical density, CE: coefficient of error, AP: anteroposterior, L: lateral, DV: Dorsoventral, PFA: paraformaldehyde, PBS: Phosphate buffered saline, SURS: systematic uniform random sampling

Key Words: Parkinson's disease, Substantia nigra, Striatum, 6-hydroxydopamine, Spatial arrangement, Stereology

Send correspondence to: Yousef Sadeghi and Mohammad Amin Abdollahifar, Department of Biology and Anatomical Sciences, School of Medicine, Shahid Beheshti University of Medical Sciences, Tehran, Iran, Tel: 98-2122439976, Fax: 98-2122439976, E-mail: mohammadaminabdollahifar@gmail.com